

Review | Received 18 October 2024; Accepted 12 February 2025; Published 27 February 2025
<https://doi.org/10.55092/aimat20250006>

Structures and mechanical properties of high-entropy carbides ceramics calculated based on first-principles

Jingyi Guan¹, Xin Zhao¹, Shangshang Fang¹, Yang Liu², Xiaobei Zang¹, Bo Wang^{3,4,*} and Ning Cao^{1,*}

¹ Shandong Key Laboratory of Intelligent Energy Materials, School of Materials Science and Engineering, China University of Petroleum (East China), Qingdao 266580, China

² Expert Workstation of Carbon-based Functional Materials Research Center, Qingdao Shichuang Technologies Co., Ltd., Qingdao, 266000, China

³ School of Materials Science and Chemical Engineering, Harbin Engineering University, Harbin, 150001, China

⁴ Qingdao Innovation and Development Center, Harbin Engineering University, Qingdao, 266000, China

* Correspondence authors; E-mails: wbheu@hrbeu.edu.cn (B. W.); caoning@upc.edu.cn (N. C.).

Highlights:

- First-principles calculations predict mechanical properties of high-entropy carbide ceramics.
- Structural stability and lattice distortion effects on carbide ceramics are analyzed.
- Comprehensive review of high-entropy carbide crystal structure by first-principles theory.

Abstract: High-entropy carbide ceramics (HECCs) materials that are made up of more than four metal carbides, have great significances in the field of ultra-high temperature service environment because of their great thermal stability. Compared with single metal carbides, HECCs materials involve complicated combination of ingredients, multiple scale dimensions design and multi-field coupling service environment, accompanying with an inefficient developing by traditional empirical trial-and-error method. Fortunately, with the development of computational materials science, multi-scale simulation calculation methods improve the research and application efficiency of HECCs. This work briefly summarized the principle and calculation process of the representative first-principles calculations method, and then reviewed the usability in the estimation of composition stability, structural design and mechanical property of HECCs. Finally, the prospect of the first-principles calculation method in the study of HECCs was prospected.

Keywords: high-entropy carbides ceramics; first-principles calculation; phase stability; mechanical properties



Copyright©2025 by the authors. Published by ELSP. This work is licensed under Creative Commons Attribution 4.0 International License, which permits unrestricted use, distribution, and reproduction in any medium provided the original work is properly cited.

1. Introduction

The high-entropy ceramics (HECs) were developed according to high-entropy alloys (HEAs) whose concept was initially introduced by Ye. *et al* [1] in 2004. At the same time, Cantor *et al.* [2] also came up with the concept of multi-principal element alloys (MPEAs). Both HECs and HEAs are single-phase solid solutions prepared from a variety of metal elements (more than four) in equal molar ratio or close to equal molar ratio. Coincidentally, good structural stability, excellent mechanical properties and functional properties are achieved by maximizing the configuration entropy.

Stefano's team [3] from North Carolina State University in the United States successfully prepared $(\text{Mg}_{0.2}\text{Co}_{0.2}\text{Ni}_{0.2}\text{Zn}_{0.2}\text{Cu}_{0.2})\text{O}$ oxide HECs for the first time in 2015, which triggered the research boom of HECs. Compared with traditional ceramics, HECs show excellent properties, such as high hardness, high modulus, low thermal conductivity and good oxidation resistance, mainly owing to the four major effects of high-entropy materials [4–7].

High-entropy carbide ceramics (HECCs) materials based on refractory metal carbide ceramics have become one of the research hotspots because of elevated melting temperatures, superior elevated-temperature mechanical robustness, notable heat resistance and minimal thermal expansion. Considering the complex composition space of HECCs materials, it is too inefficient to develop high-performance HECCs materials by scientific intuition and empirical trial-and-error traditional research methods, which comes with a long term of development and application cycle. However, with the development of computational science and artificial intelligence technology, materials science has gradually moved from an empirical science to a rational science. Multi-scale material calculation methods have become one of the fast and accurate methods to predict the structure and properties of HECCs, which can effectively reduce resource waste and environmental pollution simultaneously, such as the simulation calculation based on first-principles [8–14].

At present, there have been many reports on the prediction of HECCs based on first-principles calculation. Considering the application background of HECCs, the research mainly covers the influence of the number and types of components, and the change of metal components on the mechanical, thermal and other functional properties. However, the formation ability of high entropy single-phase and the effects of lattice distortion on mechanical properties have not been summarized by the first principles methods in detail. In this work, the method and the research progress of the first-principles calculation in the composition screening, and structural and mechanical properties prediction of HECCs have been summarized. Meanwhile, the prospect of the first-principles calculation method in the study of HECCs is also prospected in this paper.

2. High-entropy carbide ceramics

Conventional single-phase high-entropy carbide ceramics (HECCs) typically consist of four or more transition metal carbides (e.g., TiC, HfC, ZrC, TaC), where carbon atoms occupy octahedral interstitial positions within a face-centered cubic (FCC) lattice formed by transition metals, and the crystal structure decided by one of the original single carbides as well as lattice distortion results in the desirable performance of HECCs [15–20]. Thus, the properties of single metal carbide are very important for the design of HECCs. The crystal structure, lattice parameters, melting point and formation enthalpy of common single transition metal carbides are shown in Table 1.

For HECCs, the metal components atoms of (Ti, Zr, Hf, Nb, Ta)C solid solution occupy the lattice positions, and carbon atoms take over the interstitial positions [21–23]. Interestingly, most transition metal carbides have a Na-Cl structure (Figure 1). The enthalpy of formation in HECCs exhibits a strong dependence on the specific metal elements involved, with the absolute value decreasing as the atomic number of the constituent metals increases, and each atom is surrounded by eight closest atoms [24]. In addition, metallic, covalent, and ionic bonds together constitute the bonds of transition metal carbides whose metallic bonds results from non-zero electrons in some Fermi energy states [25].

Table 1. Common physical parameters of single transition metal carbides.

Compound	Crystal structure	Lattice parameter, Å	Melting point, °C	Formation enthalpy, kcal/mol
TiC ^[14,24,26]	FCC	4.333	3067	-44.0
ZrC ^[14,24,26]	FCC	4.710	3420	-47.0
HfC ^[14,26]	FCC	4.637	3928	-60.1
NbC ^[14,24,26]	FCC	4.482	3600	-33.2
TaC ^[14,26]	FCC	4.452	3950	-35.0
VC ^[14,24,27]	FCC	4.157	2830	-10.9
WC ^[14,28]	HCP	-	2867	-9.69
CrC ^[29,30]	FCC	4.016	-	15.8
MoC ^[31,32]	FCC	4.390	-	13.1

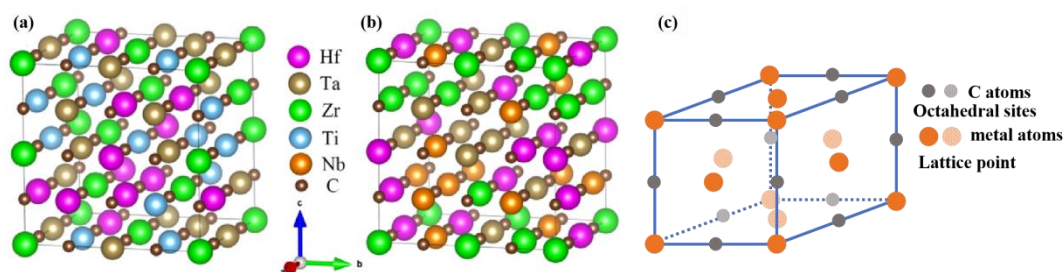


Figure 1 Crystal structure model of transition metal carbides with salt rock structure [33] Reprinted with permission [33]. Copyright 2020 Wiley: (a) and (b) are different stochastic models with the same atoms; (c) Schematic diagram of unit cell crystal structure.

The melting point of transition metal carbides is often above 3000 °C (as seen in Table 1), and they have so good thermal properties, mechanical properties and chemical stability that they are widely used in extreme environments, such as the nose cone of high-speed aircraft. The enthalpy of formation in HECCs exhibits a strong dependence on the specific metal elements involved, with the absolute value decreasing as the atomic number of the constituent metals increases. While, the absolute formation enthalpy of the same group increases with the atomic number of the metal. In addition, the basic properties of transition metal carbides combine the characteristics of metals and ceramics under the joint action of strong metallic, covalent and ionic bonds [34–36]. Since metal atom sites can be occupied by a variety of elements in the IVB-VIB groups, and nonmetal sites can also be occupied by one or more elements, it greatly increases the selectivity and complexity of high-entropy carbide components [37–39].

Fortunately, the structure and properties of HECCs can be predicted using the material computation methods based on the composition.

3. The first-principles calculation and simulation of HECCs

Material integration computing technology can not only greatly reduce the repetitive and trial-and-error work in the development process of HECCs materials, but also accelerate the theoretical innovation in the process of material research, so as to accelerate the development and application process of HECCs materials.

First-principles calculations, also known as ab initio calculations, are a method based on quantum mechanics principles. This method is not to depend on experimental data or empirical parameters, but to directly begin with the fundamental equations of quantum mechanics and computational approaches rooted in quantum mechanical principles offer a methodology independent of empirical parameters or experimental datasets, particularly those solving the Schrödinger equation to derive system properties [11,40–44] (as shown in Equation (1)).

$$\hat{H}\Psi(r, R) = E_H\Psi(r, R) \quad (1)$$

where, Ψ is the wave function; E is the ground state energy of the system; \hat{H} is the Hamiltonian operator; \vec{r} is the set of coordinates for all electrons; \vec{R} is a set of coordinates of the nucleus.

Density functional theory (DFT) that has emerged as a predominant computational framework in the physical chemical field is a simulated calculation method of the relationship between electron, nucleus and their movements through quantum mechanics [12]. DFT is grounded in the Hohenberg-Kohn theorem and Kohn-Sham equations [44,45], which can be used relatively few calculations for higher accuracy by solving the electron density to determine the structural quality of the material, and the latter calculation process is shown in Figure 2.

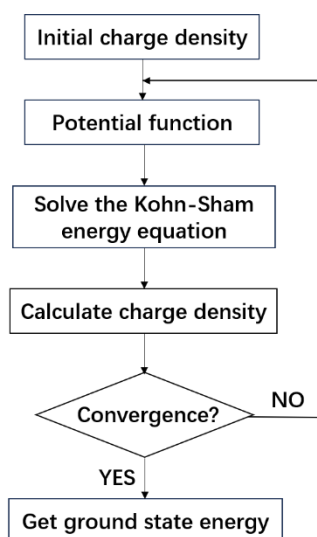


Figure 2 Flow chart illustrating a self-consistent solution to the Kohn-Sham equation [45].

Based on DFT, its predictive accuracy hinges critically on approximations for the exchange-correlation potential, commonly addressed through Local Density Approximation (LDA) or Generalized Gradient Approximation (GGA) methods [40,45,46]. These techniques are frequently implemented in software packages such as the Vienna Ab initio Simulation Package (VASP) [47–49], CASTEP [46,50], Quantum Espresso [51], Abinit [52] and so on. For instance, Liu *et al.* [50] employed the GGA-PBE (Perdew-

Burke-Ernzerhof) formalism within CASTEP to assess mechanical properties, lattice discrepancies, and structural stability across fifteen HECCs, demonstrating their exceptional characteristics including extreme hardness, fracture resistance, and ultra-high melting points (Figure 3 (a)). Liu *et al.* [53] studied the thermal as well electrical properties of $(\text{Ti}_{0.2}\text{Zr}_{0.2}\text{Nb}_{0.2}\text{Hf}_{0.2}\text{Ta}_{0.2})\text{C}$ using the CASTEP based on DFT, predicting the room temperature conductivity through experiments successfully (Figure 3(b)). Through first-principles calculation integrated with simulations and experimental analyses, in their study of $(\text{Ti}_{0.2}\text{V}_{0.2}\text{Nb}_{0.2}\text{Ta}_{0.2}\text{W}_{0.2})\text{C}_x$ high-entropy carbide synthesis, Ouyang *et al.* [46] proposed an anionic vacancy filling (AVF) mechanism to explain structural evolution, as illustrated in Figure 3(c). Employing first-principles calculations via the GGA approach in Quantum Espresso v6.2, Hossain *et al.* [51] explored carbon concentration dependent mechanical behavior in $(\text{HfNbTaTiZr})\text{C}_x$ thin films.

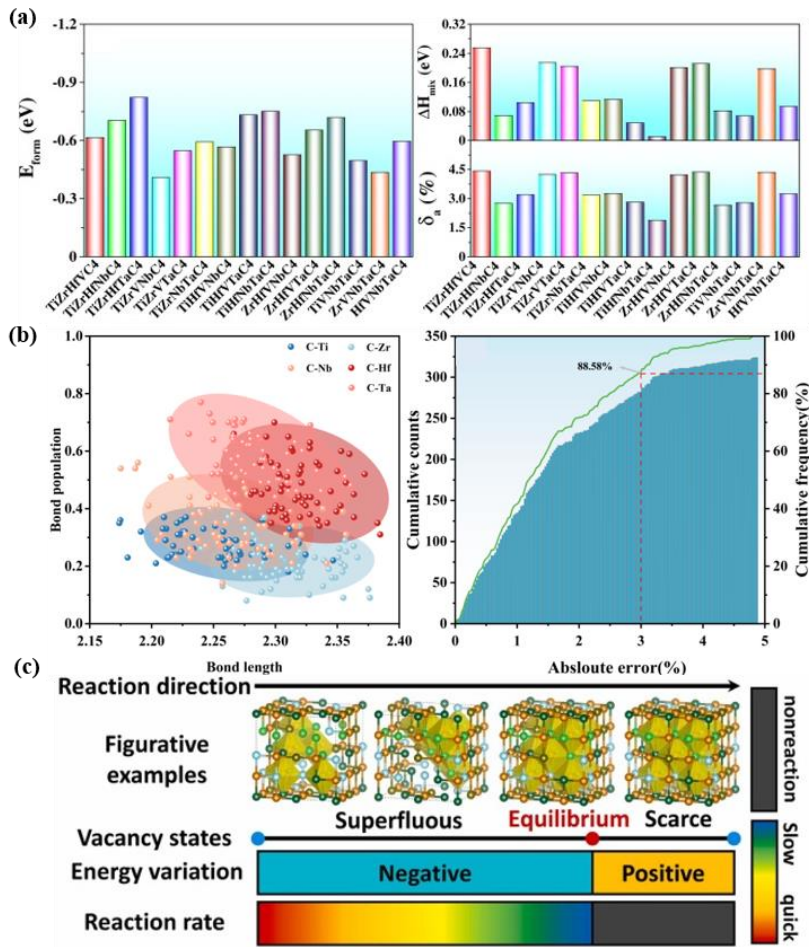


Figure 3. Different calculations of HECCs by first-principle: (a) The formation energy (E_{form}), mixing enthalpy (ΔH_{mix}) and lattice constant difference (δ_a) of fifteen HECCs [50]. Reprinted with permission [50]. Copyright 2021 Elsevier; (b) The bond population (BP)-bond length (BL) of each bond, and the absolute error (%) between M-C in HECCs and TaC in binary carbide [53]; (c) Energy variation state and reaction rate of $(\text{Ti}_{0.25}\text{V}_{0.25}\text{Nb}_{0.25}\text{Ta}_{0.25})\text{C}_x$ [46]. Reprinted with permission [46]. Copyright 2024 Elsevier.

In addition, based on the electronic structure characteristics of HECCs system, it is not only able to obtain the electronic state density and the structure affected by lattice distortion, but also the ability to predict the properties of the material, such as mechanical, thermal physics, optical, electrical, *etc.*, to

select the component system of the target energy and improve the development efficiency of HECCs materials [46,50,54]. In general, the calculation time is proportional to the size of the supercell. Limited by the processing capacity of the computer, the material system that can be processed is relatively small, usually less than one hundred [46,49,51,53]. At present, researchers successfully predicted the production of components, structures, single-phase high-entropy formation ability and basic mechanical properties of HECCs based on the first-principles calculation [55–58].

4. Phase and structure of HECCs

4.1. Phase stability evaluation and crystal structure of HECCs

Hundreds of HECCs (more than four kinds of metal elements) have been found, and some crystal structures and unit cell parameters are shown in Table 2. Different transition metal sizes, and the different crystal structure, lattice size and electron distribution of binary carbides cause differences of stability and formation ability of HECCs solid solution [55–59].

Table 2. Component design and crystal structure of HECCs solid solution.

Component	Crystal structure	Lattice constants, a = b = c
(TaNbHfZrTi)C ^[55]	FCC	4.528
(HfZrTaNbTi)C ^[7]	FCC	4.528 ± 0.005
(ZrNbTiV)C ^[24]	FCC	4.434
(HfTaZrTi)C ^[33]	FCC	4.554
(HfTaZrNb)C ^[33]	FCC	4.583
(TiZrHfCr)C ^[56]	FCC	4.487
(TiZrHfMo)C ^[56]	FCC	4.524
(TiZrHfW)C ^[56]	FCC	4.513
(TiZrVCr)C ^[56]	FCC	4.353
(TiZrVMo)C ^[56]	FCC	4.410
(TiZrVW)C ^[56]	FCC	4.400
(TiZrNbCr)C ^[56]	FCC	4.437
(TiZrNbMo)C ^[56]	FCC	4.480
(TiZrNbW)C ^[56]	FCC	4.480
(NbTaZrW)C ^[57]	FCC	4.509
(NbTaZrHfW)C ^[57]	FCC	4.5285
(TaNbTiZr)C ^[58]	FCC	4.504
(TaNbTiZrHf)C ^[58]	FCC	4.534
(TaNbTiZrHfMo)C ^[58]	FCC	4.504
(TaNbTiZrHfMoV)C ^[58]	FCC	4.464
(TaNbTiZrHfMoVW)C ^[58]	FCC	4.455
(TaNbTiV)C ^[34]	FCC	4.376
(ZrNbTaHf)C ^[59]	FCC	4.563
(ZrNbTaHfTi)C ^[59]	FCC	4.553
(ZrNbTaHfTiV)C ^[59]	FCC	4.495

4.1.1. Criterion of mixed Gibbs free energy

Because of the scale and the number of elements, there is a wide design space of HECCs. In order to effectively select the atomic combination of single-phase HECCs, the researchers constantly develop the new body, and try to predict the formation ability through theoretical calculation.

Gibbs free energy serves as a key criterion for evaluating thermodynamic stability in single-phase high-entropy ceramic systems [24]. For high-entropy carbide ceramics, this stability is fundamentally linked to the combined Gibbs free energy (ΔG_{mix}), a parameter quantitatively described in Equation (2),

$$\Delta G_{\text{mix}} = \Delta H_{\text{mix}} - T\Delta S_{\text{mix}} \quad (2)$$

Here, ΔH_{mix} and ΔS_{mix} denote the enthalpy and entropy of mixing for HECC systems, respectively. A negative ΔG_{mix} ($\Delta G_{\text{mix}} < 0$) indicates a possible stabilized solid solution [24,60]. Equation (3) provides the computational framework for determining zero-temperature/pressure mixing enthalpy (ΔH_{mix} at 0 K and 0 Pa) in HECCs.

$$\Delta H_{\text{mix}}^{0\text{K}} = E_{\text{HECCS}} - (E_{\text{TM1C}} + E_{\text{TM2C}} + E_{\text{TM3C}} + E_{\text{TM4C}} + E_{\text{TM5C}}) / 5 \quad (3)$$

E represents density functional theory (DFT)-derived energies for both constituent transition metal carbides (TM1C-TM5C) and the resultant HECC phase. The positive and negative values of $\Delta H_{\text{mix}}^{0\text{K}}$ determine whether it is an endothermic or exothermic process. In addition, there are two sublattices for HECCs where h represents the metallic sites and k denotes the carbon sites. Their configurational mixing entropy can be formulated through Equation (4) [24,61],

$$\Delta S_{\text{mix}} = -R \left\{ \frac{X}{X+Y} \sum_{i=1}^{N_h} x_i^h \ln(x_i^h) + \frac{X}{X+Y} \sum_{i=1}^{N_k} x_i^k \ln(x_i^k) \right\} \quad (4)$$

where, N_h and N_k correspond to elemental diversity within sublattices h and k , while molar fractions of component i in these sublattices are denoted by respective variables.

Further considering the carbon vacancy properties of HECCs, the actual configuration is that the metal atoms randomly occupy the metal sublattice, while the carbon atoms and a certain concentration of vacancy occupy the carbon sublattice, so the mixed entropy of HECCs comes from the disorder of the metal sublattice and the vacancy in the carbon sublattice [24,61]. For example, Ye research group [24,55] has verified through experiments that (ZrNbTiV)C carbide has dual sublattice structure characteristics: in the carbon sublattice system, the atomic sites show a statistical distribution of carbon atoms and vacancy accounting for 50% each, while the metal sublattice is occupied by four or more transition group elements in disordered solid solution form. It is particularly noteworthy that the vacancy defects in the carbon sublattice can be equivalent to the virtual components participating in the entropy calculation, and this unique structural design significantly improves the configuration entropy of the carbon sublattice. Therefore, the overall mixing entropy of the material contains two dimensional contributions, including the synergistic superposition effect of the multi-element disorder distribution of the metal sublattice and the vacancy defect entropy of the carbon sublattice. The different ΔS_{mix} of no vacancies and 50% carbon vacancies are 0.693R and 1.040R, respectively. In the case of the DFT, using Special Quasi-random Structure (SQS) modeling, Ye *et al.* [7] quantified both mixing enthalpy and configurational entropy for (TiZrHfNbTa)C systems, and determined the stable temperature of the mixed Gibbs freedom for the negative (TiZrHfNbTa)C using thermodynamic data, which is the guide to the synthesis of this HECCs.

4.1.2. Criterion of entropy formation ability

Entropy Forming Ability (EFA) was used to predict whether multi carbides can form single phase based on the first-principles calculations [8]. Entropy estimation involves analyzing the metastable energy spectrum (H) relative to the ground state, with standard deviation σ inversely correlating with entropy magnitude S . For a system without specific species, the descriptor (EFA) is defined as $1/\sigma$, measured above the ground state of the system at absolute zero temperature. The calculation expression is shown in the Equation (5) and (6),

$$EFA(N) \equiv \left\{ \sigma [\text{spectrum}(H_i(N))]_{T=0} \right\}^{-1} \tag{5}$$

$$\sigma \{Hi(N)\} = \sqrt{\frac{\sum_{i=1}^n g_i (H_i - H_{mix})^2}{(\sum_{i=1}^n g_i)^{-1}}} \tag{6}$$

Here, n indicates geometric configuration multiplicity, g_i reflects degeneracy states, and H_{mix} is derived from enthalpy-weighted averaging across configurations (Equation (7)),

$$H_{mix} = \frac{\sum_{i=1}^n g_i H_i}{\sum_{i=1}^n g_i} \tag{7}$$

Sarker *et al.* [8] calculated EFA values for a total of fifty-six five-membered carbides and some of them were tested by experimental verification as shown in Table 3. Elevated values correlate strongly with single-phase solid solution formation in pentenary carbides, aligning with an established EFA synthesis threshold of $50 \text{ (eV/atom)}^{-1}$. The five-membered carbides with a large EFA value all form single-phase solid solution, while the second phase is easy to appear in the five-membered carbides with small EFA value [8,9], as shown in Figure 4. In addition, Kaufmann *et al.* [14] predicted EFA values of seventy kinds of five-membered carbides containing Group VI elements through machine learning, and verified several typical compositions in combination with experiments, further confirming the effectiveness of EFA model in high-throughput exploration of high-entropy ceramic compositions (Table 3).

Table 3 EVA values of different HECCs by first-principles calculations.

Composition	EVA	Phase	Composition	EVA	Phase
(VNbTaMoW)C ^[8]	125	S	(TiZrHfMoW)C ^[8]	38	M
(TiZrHfNbTa)C ^[8]	100	S	(ZrHfVMoW)C ^[8]	37	M
(TiHfVNbTa)C ^[8]	100	S	(CrMoNbVW)C ^[14]	100	S
(TiVNbTaW)C ^[8]	77	S	(CrMoNbTaW)C ^[14]	104	S
(HfNbTiVZr)C ^[8]	71	—	(CrMoTaVW)C ^[14]	103	S
(TiHfNbTaW)C ^[8]	67	S	(CrMoTiVW)C ^[14]	88	S
(TiZrHfTaW)C ^[8]	50	S	(CrHfTaWZr)C ^[14]	51	M
(ZrHfTaMoW)C ^[8]	45	M	(CrMoTiWZr)C ^[14]	49	M
(HfTaVWZr)C ^[8]	43	—	(CrHfMoTiW)C ^[14]	45	M

Notes: *S: Single-phase; M: Multi-phase.

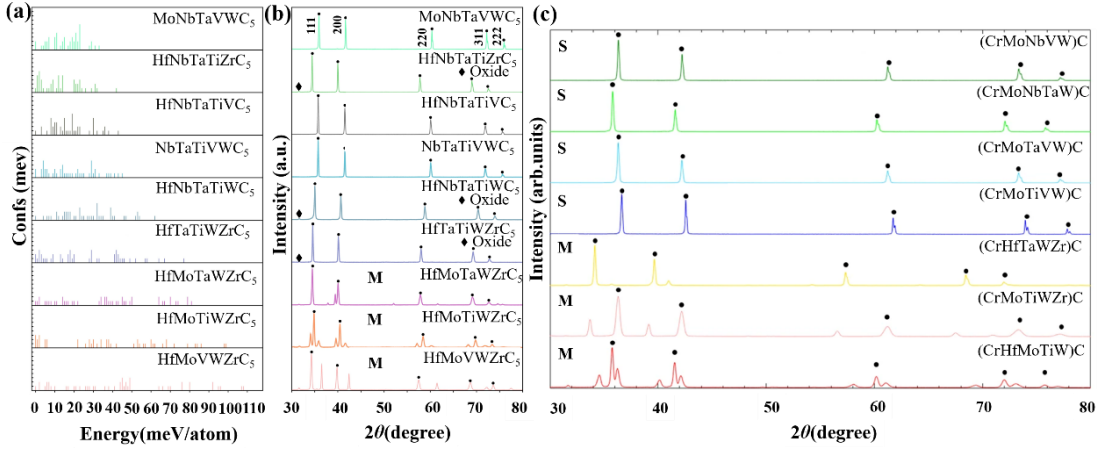


Figure 4. The energy distribution and XRD diffraction pattern of different configuration, while (a) and (b) are from Reference [8], and (c) is from Reference [14], and comparative analyses include (a) configuration energy profiles for nine pentenary carbides, (b) XRD patterns of these nine systems, and (c) diffraction data for seven analogous compositions.

4.1.3. Criterion of lattice constant difference

Single-phase HECC formation propensity depends critically on constituent atomic radii, quantified through lattice mismatch parameter δ , and δ less than or equal to 6.6% is easy to form a single phase. For multicomponent solid solutions, δ can be determined by Equation (8) [62],

$$\delta = \sqrt{\sum_{i=1}^n n_i c_i \left(1 - \frac{r_i}{\bar{r}}\right)^2} \quad (8)$$

where, c_i and r_i correspond to the atomic fraction and the lattice constant of i atom, respectively, while \bar{r} is the average lattice constant of n components.

For example, Ning *et al.* [34] performed DFT calculation by VASP, based on the δ as the criterion of single-phase formation. The results showed that (TaNbTiV)C has a smaller δ about 3.014%, indicating a smaller degree of lattice distortion, which increases the possibility to form a single-phase solid solution. In addition, the negative ΔH_{mix} observed in (TaNbTiV)C systems thermodynamically favors single-phase solid solution formation. The experiment results that metal carbides with single phase rock salt structure were synthesized also confirm the reliability of the first-principles calculations [24,55].

However, although there are different methods to predict the formation ability of HECCs, there is not a universal parameter to apply to all kinds of HECCs, which is independent of the number of metal or nonmetal elements. It is also one of the directions that needs to develop for high-entropy ceramics.

4.2. Electronic structure

Bonding characteristics, lattice distortion, as well as the microscopic mechanism of its structural stability and mechanical properties can be expressed by the electronic structure of materials. For (HfTaZrTi)C and (HfTaZrNb)C HECCs [63], both them have similar shape and position to Density of States (DOS) peaks (Figure 5). In addition, the DOS at the Fermi level has some values, meaning the presence of metallic bonds, which is similar to the single-transition-metal carbide [25,26]. Near the Fermi level, their

state density is mainly produced by the p-orbital electrons of C atoms and d-orbital electrons of metal atoms, which form covalent bonds. The more electron transfer indicates a stronger ionic property in (HfTaZrTi)C, while a stronger covalent bond in (HfTaZrNb)C. Similarly, Zhang *et al.* [65] also found that there are strong covalent bonds of ionic and metallic characteristics in (TiZrHfNbTa)C as a positive effect on its mechanical strength (Figure 5 (c)). Thus, HECCs have so complex bonding characteristics that the analysis of electronic structure is of great significance to the prediction of structural stability as well as mechanical properties.

For example, the mechanical properties, thermal stability, and chemical stability of HECCs are affected by the changes in electronic structure directly. In addition, because the bonding strength between metal atoms and carbon atoms affects the formation ability and hardness of the material, the types and proportions of metal side elements can control the mechanical properties. In addition, the replacement of metal elements may lead to changes in the amount of charge transfer, thereby affecting the brittleness and toughness of the material.

At present, researches are focus on the effects of different electron orbitals on bonds for HECCs. However, there is not a detailed statistical data about the kinds and contents of different bonds for different HECCs. In addition, the relationship between the content of bonds and the types of metal components, as well as the mole ratios of metal and nonmetal, has not been reported in detail.

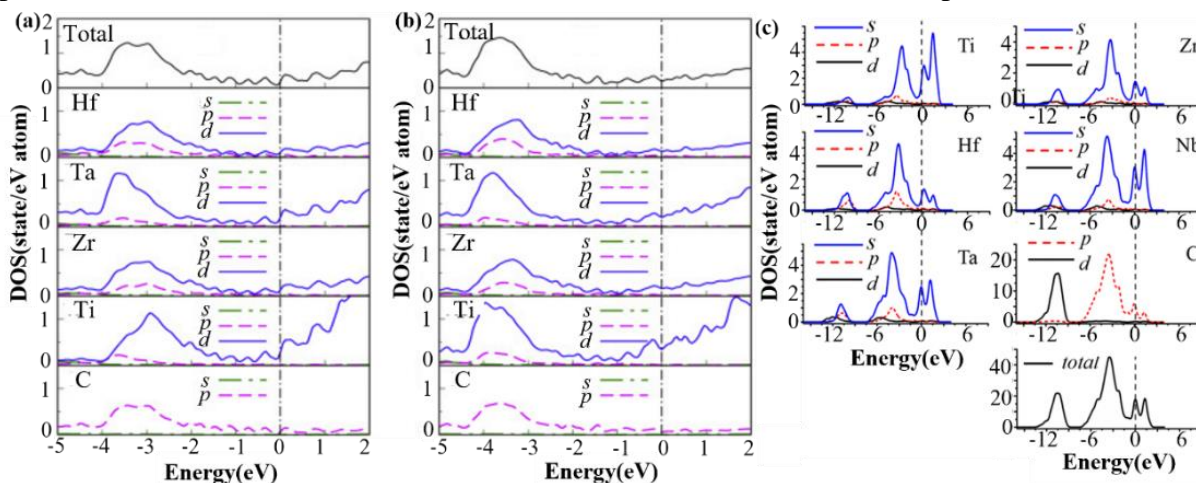


Figure 5. DOS of high-entropy carbides ceramics [63,65]. Reprinted with permission [63]. Copyright 2020 Elsevier. Reprinted with permission [65]. Copyright 2019 American Institute of Physics: (a) (HfTaZrTi)C; (b) (HfTaZrNb)C; (c) (TiZrHfNbTa)C.

4.3 Lattice distortion

Lattice distortion has an important effect on high-entropy materials, which is caused by the mismatch of atomic sizes of high concentration component elements [59,66,67]. The study of lattice distortion in HECCs is a great help to comprehend the strengthening mechanism of their excellent mechanical properties.

Sun *et al.* [68] proposed that the vacancy formation energy of high-entropy ceramics is positively correlated with lattice distortion. Double carbon vacancy formation energy of (NbTaCrTiVZr)C₆, (WCrTaTiVZr)C₆, (NbTaWCrVZr)C₆ and (CrMoTaVWZr)C₆ systems which have highly lattice distortion is more than that of (CrMoNbTiVW)C₆, (MoTaCrTiVW)C₆, (MoVWTiNbTa)C₆ and (MoWTiZrNbTa)C₆ systems whose lattice distortion is smaller. In addition, the system with large lattice

distortion is not easy to produce carbon vacancy, and this phenomenon manifests with particular prominence in metallic vacancy formation energies, as these demonstrate heightened sensitivity to variations in lattice distortion magnitude.

In addition, high pressure can lead to changes in material structure and properties [69–72]. Given that high-entropy ceramic carbides (HECCs) predominantly operate under extreme thermomechanical conditions (elevated temperatures > 1000 °C and pressures > 5 GPa), understanding pressure-dependent elastic behavior becomes crucial for performance evaluation [73,74]. Through density functional theory simulations, Yang's group [47] systematically investigated the pressure-modulated elastic response evolution in (TaNbHfTiZr)C systems. The results showed that HECCs have the mixed characteristics of covalent bond and ionic bond, and ionic bond was stronger under pressure, and tough-brittle transition was also showed in the HECCs when the pressure was at 20 GPa. Complementary research by Jiang *et al.* [33] employed Ab initio molecular dynamics to characterize the pressure-induced mechanical evolution pathways in both (HfTaZrTi)C and (HfTaZrNb)C compounds, revealing distinct pressure-hardening mechanisms between the two material systems. The results showed that the chemical bonds formed by C and transition metals tended to be covalent with the pressure increases, following the decrease of hardness, lattice parameters and elasticity modulus. Complete and detailed research by Xiong *et al.* [48] studied the influence of pressure on the crystal stability, mechanical properties and electronic structure of (TiZrNbTa)C whose lattice parameters and brittleness decreased and elastic constant and elastic modulus increased with the increase of pressure. Figure 6 showed the crystal structure and grain boundary with lattice distortion under pressure.

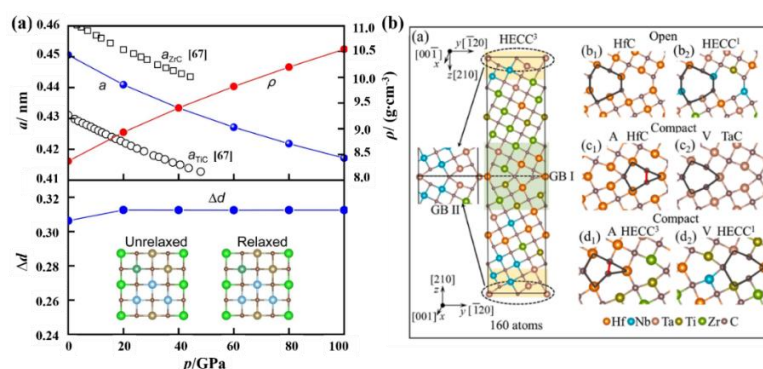


Figure 6. Models of local lattice distortion [48,74]. Reprinted with permission [48]. Copyright 2021 Springer. Reprinted with permission [74]. Copyright 2024 Elsevier: (a) lattice parameter, density and the variation law of local lattice distortion with pressure; (b) lattice distortion of HECCs at grain boundaries.

Lattice distortion can change the stress field and elastic strain energy inside the material, resulting in strain strengthening effects. Therefore, the increase of lattice distortion can improve the hardness and toughness of HECCs. However, excessive lattice mismatch leads to increased brittleness. Besides, lattice distortion directly affects the stability of HECCs, which can be reified as a small lattice distortion meaning a well stability and a significant one corresponding to a poor stability, and even lead to phase transitions at high temperatures.

5. Mechanical properties of HECCs by first-principles calculations

Elastic properties offer fundamental insights into the mechanical behavior of materials. In engineering contexts, changes in elastic properties under varying environmental conditions are frequently observed, and understanding the pressure dependence of these properties is essential for predicting how pressure influences mechanical stability and associated fundamental physical characteristics [74,75]. Typically, the elastic constants of a cubic lattice (C_{11} , C_{12} , and C_{44}) are determined via the strain-stress method [76]. Employing the generalized Born's framework, the thermodynamic stability criteria for cubic crystalline systems subjected to hydrostatic compression are mathematically formalized through Equation (9), establishing critical boundaries for lattice integrity preservation [77],

$$C_{11} - P > 0, C_{44} - P > 0, C_{11} - C_{12} - 2P > 0, C_{11} + 2C_{12} + P > 0. \quad (9)$$

The modules, Poisson's ratio, Platts' ratio and Vickers hardness of HECCs can be calculated from the elastic constants to evaluate their elastic properties. For instance, in the case of $(\text{Ti}_x\text{Zr}_{0.2}\text{Nb}_{0.2}\text{Ta}_{0.2}\text{Mo}_{0.4-x})\text{C}$ high-entropy carbides with a cubic crystal structure, the strain-stress method was employed to determine three independent elastic constants [24]. Critical elasticity parameters including B , G , and H_v were computationally resolved through constitutive relationships defined in Equations (10–15), employing tensor transformation protocols [78].

$$B = \frac{C_{11} + 2C_{12}}{3} \quad (10)$$

$$G = \frac{G_V + G_R}{2} \quad (11)$$

$$G_V = \frac{3C_{44} + C_{11} - C_{12}}{5} \quad (12)$$

$$G_R = \frac{5(C_{11} - C_{12})C_{44}}{4C_{44} + 3(C_{11} - C_{12})} \quad (13)$$

$$E = \frac{9BG}{3B + G} \quad (14)$$

$$H_v = 2(k^2G)^{0.585} - 3 \quad (15)$$

where B is bulk modulus, G is shear modulus, and k is the G/B ratio. The larger the B , the stronger the material's resistance to volume deformation under pressure; The greater the E , the stronger the resistance to unidirectional axial tensile; The greater the G , the stronger the resistance to shear strain; Moreover, Poisson's ratio and Platts' ratio serve as critical indicators to quantify the material's propensity for ductile versus brittle fracture modes.

From multiscale investigations about the computational and experimental studies, HECCs have higher hardness and modulus than single-component carbides that are calculated based on the Rule of Mixture (ROM) [8,48]. The calculation results of elastic modulus, Poisson's ratio and Przewalski's ratio of some carbide high-entropy ceramics are listed, as shown in Table 4. In addition, lattice distortion also leads to differences in elastic modulus. For $(\text{NbTaTiZr})\text{C}$ ceramics, lattice distortion results in an increase in elastic modulus, while that of $(\text{NbTiVZr})\text{C}$ ceramics is significantly reduced due to lattice distortion. At present, the prediction of elastic properties of HECCs by first-principles method has been recognized by many researchers, and computational predictions demonstrate strong congruence with empirical measurements, validating the implemented multiscale modeling framework [50].

Table 4. Calculation results of B , G , E , ν and k of HECCs

Components	B / GPa	G / GPa	E / GPa	ν	k
(HfTaZrNb)C ^[33]	270.4	205.2	485.6	0.2	1.3
(HfTaZrTi)C ^[33]	255.1	164.7	405.9	0.23	1.6
(HfTaTiWZr)C ₆ ^[8]	274	191	466	-	-
(TiZrNbTa)C ^[48]	254	466	195	0.194	1.303
(NbTaTiZr)C ^[79]	250	177	429	0.213	1.410
Lattice distortion					
(NbTaTiZr)C ^[79]	264	189	458	0.211	1.397
(NbTiVZr)C ^[79]	270	197	476	0.206	1.370
Lattice distortion					
(NbTiVZr)C ^[79]	274	203	489	0.203	-
(HfZrTaNbTi)C ^[47]	264.5	179.6	439.4	0.223	1.47
Lattice distortion					
(TiZrHfTaNb)C ^[80]	241.29	185.82	44.09	0.193	1.29
(TiZrHfTaMo)C ^[80]	255.67	181.11	439.55	0.213	1.41
(TiZrHfTaV)C ^[80]	241.54	178.73	430.10	0.203	1.35
(TiZrHfTaCr)C ^[80]	230.90	171.36	412.14	0.203	1.35
MoNbTaVWC ₅ ^[8]	312	183	460	-	-
HfNbTaTiZrC ₅ ^[8]	362	192	464	-	-
HfNbTaTiVC ₅ ^[8]	276	196	475	-	-
HfNbTaTiWC ₅ ^[8]	291	203	493	-	-
NbTaTiVZrC ₅ ^[8]	305	199	490	-	-
HfNbTiWZrC ₅ ^[8]	274	191	466	-	-

Li *et al.* [81] found that the ratio and arrangement of metal atoms significantly influence the mechanical properties and slip mechanisms. IVB group transition metal carbides tend to slip along (110)/[110], when VB group transition metal carbides tend to slip along (110)/[111]. The quasi-equilibrium mechanical response of (HfTiZr)_{1-x}(NbTa)_xC adheres to established composite material blending laws. However, atomic-scale bond strength analysis reveals yield shear stress is predominantly dictated by Me-C bond dissociation energies at active slip planes, whose spatial orientation correlates with γ -surface minima in stacking fault energy landscapes. As evidenced in Figure 7, the average lattice constants and modules of (HfTiZr)_{1-x}(NbTa)_xC means that the change of atom type and content can affect the lattice constant and modules directly, as well as a good agreement with the ROM method. Moreover, when $x > 0.5$, dissociation takes place on the (111) slip plane, suggesting that the primary (110)/[110] slip system characteristic of IVB group transition metal carbides may shift to the (110)/[111] slip system. By modifying the ratio and arrangement of various group metal atoms within (HfTiZr)_{1-x}(NbTa)_xC, it is possible to tailor the material's slip behavior, yield shear strength, and plasticity.

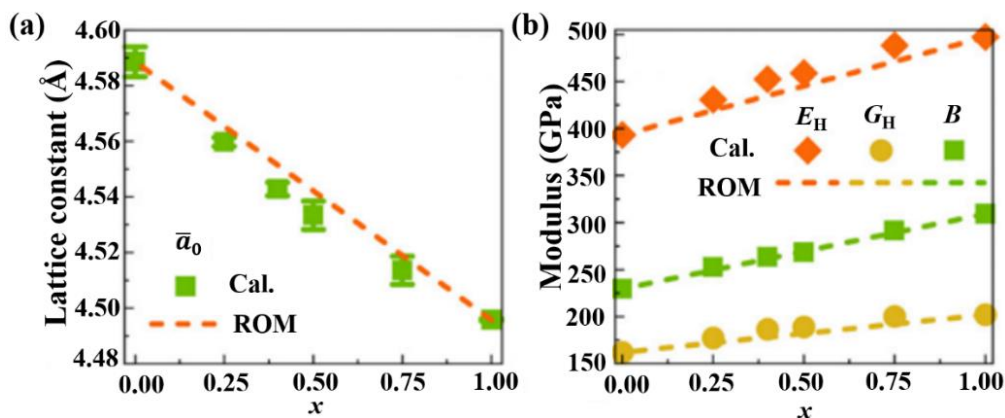


Figure 7. Average lattice constants (a) and modules (b) of $(\text{HfTiZr})_{1-x}(\text{NbTa})_x\text{C}$ and those predicted by ROM [81]. Reprinted with permission [81]. Copyright 2024 American Physical Society.

In addition, the grain boundary structure also determines the mechanical properties of HECCs. Li *et al.* [74] studied the mechanical response of $\{210\}/[001]_{\text{GB}}$ in $(\text{HfNbTaTiZr})\text{C}$ under shear deformation. The GB migrates in VB carbides, while C-C bond formed inside GB in IVB carbides inhibits GB migration, resulting in Metal-C bond breakage, as well as the failure of the super-battery. By customizing grain boundaries in $(\text{HfNbTaTiZr})\text{C}$ with metal atoms from diverse groups, a ‘pinning’ effect can be introduced, which may enhance plasticity while maintaining strength. Furthermore, high-entropy carbide ceramics (HECCs) demonstrate greater grain boundary migration stress than traditional binary carbides. These findings offer valuable insights into the mechanical properties of grain boundary structures in high-entropy carbide ceramics.

In short, the lattice distortion and grain boundary structure directly affect the mechanical properties of HECCs, which are influenced by the size and atomic proportion of transition metal atoms. Therefore, based on first-principles calculation, structural design is expected to guide the preparation of HECCs with specific mechanical properties. However, the difficulty in controlling the influencing factors of the experimental process has become a key constraint on preparation.

6. Summary and prospect

The first-principles calculation can effectively predict the crystal structure, single-phase formation ability, stability, and mechanical properties of HECCs, shorten the development cycle and avoid resources wast. Based on the first-principles calculation, multiple types of calculations can be performed regarding high entropy ceramics.

- (1) The accurate prediction and simulation of the crystal structure of HECCs based on first-principles calculation were summarized. HECCs tend to form FCC structures, and the formation ability of single-phase HECCs was tested based on different evaluation parameters;
- (2) This article summarizes the results of first-principles calculation of electronic structure information, such as band structure and DOS of HECCs which exhibits characteristics of covalent bonds, ionic bonds, and metal bonds, and the bonding strength between metal and carbon atoms varies with the type of metal atom;

(3) Based on first-principles calculation, calculation method for mechanical properties of HECCs was summarized, and the effects of pressure, lattice distortion, and grain boundary structure on the elastic modulus of HECCs were explained.

However, the first-principles calculation also has shortcomings. Due to its large amount of calculation and long-time consumption, the scale of the material system is generally about one hundred or even dozens of atoms, which is small for HECCs with disorderly distribution of various metal elements.

According to the shortcomings and advantages of first-principles calculation method, its application in HECCs should be developed in the following directions: (1) Expand the computational atomic system size and increase the number of atoms from developing more reasonable and efficient modeling and calculation methods while reducing the calculation time; (2) Integrate multi-scale calculation methods. Different properties of HECCs at different scales are studied by combining the first-principles calculations with phase molecular dynamics, machine learning, phase diagram calculation and so on; (3) Unify the calculation database results. Establish the first-principles calculations database of HECCs and standard the first-principles calculation software, so that the calculation results of different researchers are more standardized and comparable.

Acknowledgements

This work was financially supported by the Qingdao Natural Science Foundation Youth Project (project number: 24-4-4-zrjj-64-jch), the China Postdoctoral Science Foundation (project number: 2024M753620), the Heilongjiang Province Natural Science Foundation (LH2024E063), the Shandong Province Natural Science Foundation (project number: ZR2024QE276, ZR2024QE373), the Shandong Province Science and Technology based Small and Medium sized Enterprises Innovation Capability Enhancement Project (2023TSGC0777), and the Project of Marine Science and Technology Synergy Innovation Center (22-05-CXZX-04-04-29).

Authors' contribution

Conceptualization, J.G. and X.Z.; formal analysis, S.F.; investigation, B.W. and Y.L.; writing—original draft preparation, J.G.; writing—review and editing, X.Z.; funding acquisition, J.G., B.W. and N.C. All authors have read and agreed to the published version of the manuscript.

Conflicts of interests

The authors declare that they have no known competing financial interests or personal relationships that could have appeared to influence the work reported in this paper.

Reference

- [1] Yeh JW, Chen S, Lin S, Gan G, Chin TS, *et al.* Nanostructured high-entropy alloys with multiple principal elements: novel alloy design concepts and outcomes. *Adv. Eng. Mater.* 2004, 6(5):299.
- [2] Cantor B, Chang ITH, Knight P, Vincent AJB. Microstructural development in equiatomic multicomponent alloys. *Mater. Sci. Eng. A Struct. Mater.* 2004, 375–377:213–218.
- [3] Rost CM, Edward S, Trent B, Ali M, Dickey EC, *et al.* Entropy-stabilized oxides. *Nat. Commun.*

- 2015, 6(1):8485.
- [4] Zhang W, Liaw P, Zhang Y. Science and technology in high-entropy alloys. *Sci. China Mater.* 2018, 61(1):2–22.
- [5] Miracle DB, Senkov ON. A critical review of high entropy alloys and related concepts. *Acta Mater.* 2017, 122:448.
- [6] Harrington TJ, Gild J, Sarker P, Toher C, Rost CM, *et al.* Phase stability and mechanical properties of novel high entropy transition metal carbides. *Acta Mater.* 2018, 166:271–280.
- [7] Ye B, Wen T, Huang K, Wang C, Chu Y. First-principles study, fabrication, and characterization of (Hf_{0.2}Zr_{0.2}Ta_{0.2}Nb_{0.2}Ti_{0.2})C high-entropy ceramic. *J. Am. Ceram. Soc.* 2019, 102(7):4344.
- [8] Sarker P, Harrington T, Toher C, Oses C, Samiee M, *et al.* High-entropy high-hardness metal carbides discovered by entropy descriptors. *Nat. Commun.* 2018, 9:4980.
- [9] Tsai MH, Yeh JW. High-entropy alloys: a critical review. *Mater. Res. Lett.* 2014, 2(3):107.
- [10] Li J, Fang Q, Liaw PK. Microstructures and properties of high-entropy materials: modeling, simulation, and experiments. *Adv. Eng. Mater.* 2021, 23(1):2001044.
- [11] Li C, Gao R, Ouyang H, Shen T, Chen Z, *et al.* Hierarchical porous (Ta_{0.2}Nb_{0.2}Ti_{0.2}Zr_{0.2}Hf_{0.2})C high-entropy ceramics prepared by a self-foaming method for thermal insulation. *J. Adv. Ceram.* 2024, 13(7):956–966.
- [12] Anisimov VI, Aryasetiawan F, Lichtenstein AI. First-principles calculations of the electronic structure and spectra of strongly correlated systems: the LDA+U method. *J. Phys-Condens. Mat.* 1997, 9(4):767–808.
- [13] Li J, Lu F, Li T, Fu Y, Zhao J, *et al.* Superior synergistic oxidation resistance of medium-entropy carbide ceramic powders rather than multi-phase carbide ceramic powders. *J. Adv. Ceram.* 2024, 13(8):1223–1233.
- [14] Kevin K, Daniel M, Mellor WM, Zhu C, Rosengarten AS, *et al.* Discovery of high-entropy ceramics via machine learning. *Npj. Comput. Mater.* 2020, 6(1):42.
- [15] Guan J, Li D, Zhou G, Duan W, Yang Z, *et al.* Interface structure and grain growth behavior of Ta₄HfC₅-Si₂BC₃N complex ceramics. *Sci. China Mater.* 2023, 66(11):4306–4316.
- [16] Guan J, Li D, Yang Z, Cai D, Jia D, *et al.* Effect of Si₂BC₃N Additions on the oxidation of Ta₄HfC₅ ceramics at 900~1100 °C. *Corros. Sci.* 2023, 225:111585.
- [17] Guan J, Li D, Yang Z, Wang B, Cai D, *et al.* Synthesis and thermal stability of novel high-entropy metal boron carbonitride ceramic powders. *Ceram. Int.* 2020, 46:26581–26589.
- [18] Guan J, Liu Y, Li D, Yang Z, Qin S, *et al.* The new complex high-entropy metal boron carbonitride: microstructure and mechanical properties. *J. Am. Ceram.* 2022, 105(10):6417–6426.
- [19] Guan J, Li D, Yang Z, Wang B, Jia D, *et al.* Ta(B, C, N) and (Ta, Mi)(B, C, N) (Mi = Nb, W) ceramics by high-energy ball milling: processing and solution mechanisms. *J. Am. Ceram.* 2022, 106(1):699–708.
- [20] Wang B, Li D, Yang Z, Jia D, Guan J, *et al.* microstructural evolution and mechanical properties of in situ nano Ta₄HfC₅ reinforced siben composite ceramics. *J. Adv. Ceram.* 2020, 9(6):1–10.
- [21] Wang F, Zhang X, Yan X, Lu Y, Nastasi M, *et al.* The effect of submicron grain size on thermal stability and mechanical properties of high-entropy carbide ceramics. *J. Am. Ceram. Soc.* 2020, 103(8):4463–4472.
- [22] Lu K, Liu J, Wei X, Bao W, Wu Y, *et al.* Microstructures and mechanical properties of high-entropy

- (Ti_{0.2}Zr_{0.2}Hf_{0.2}Nb_{0.2}Ta_{0.2})C ceramics with the addition of SiC secondary phase. *J. Eur. Ceram. Soc.* 2020, 40(5):1839.
- [23] Ján D, Tamás C, Dávid M, Richard S; Marek V, *et al.* Nanoindentation and tribology of a (Hf-Ta-Zr-Nb-Ti)C high-entropy carbide. *J. Eur. Ceram. Soc.* 2021, 41(11):5417.
- [24] Ye B, Wen T, Nguyen MC, Hao L, Wang C, *et al.* First-principles study, fabrication and characterization of (Zr_{0.25}Nb_{0.25}Ti_{0.25}V_{0.25})C high-entropy ceramics. *Acta Mater.* 2019, 170:15–23.
- [25] Li H, Zhang L, Zeng Q, Guan K, Li K, *et al.* Structural, elastic and electronic properties of transition metal carbides TMC (TM = Ti, Zr, Hf and Ta) from first-principles calculations. *Solid State Commun.* 2011, 151:602–606.
- [26] Wright AJ, Luo J. A step forward from high-entropy ceramics to compositionally complex ceramics: a new perspective. *J. Mater. Sci.* 2020, 55(23):1–16.
- [27] Gild J, Zhang Y, Harrington T, Jiang SC, Hu T, *et al.* High-entropy metal diborides: a new class of high-entropy materials and a new type of ultrahigh temperature ceramics. *Sci. Rep.* 2016, 6(1):37946.
- [28] Zhang RZ, Reece MJ. Review of High Entropy Ceramics: Design, Synthesis, Structure and Properties. *J. Mater. Chem. A.* 2019, 7(39):22148.
- [29] Fors DHR, Wahnstrom G. Theoretical Study of Interface Structure and Energetics in Semicoherent Fe(001)/MX(001) Systems ($M = \text{Sc, Ti, V, Cr, Zr, Nb, Hf, Ta}$; $X = \text{C or N}$). *Phys. Rev. B.* 2010, 82:195410.
- [30] Xing H, Dong A, Huang J, Zhang J, Sun B. Revisiting Intrinsic Brittleness and Deformation Behavior of B2 NiAl Intermetallic Compound: A First-Principles Study. *J. Mater. Sci. Technol.* 2018, 34(4):620.
- [31] Park NY, Choi JH, Cha PR, Jung WS, Chung SH, *et al.* First-principles study of the interfaces between Fe and transition metal carbides. *J. Phys. Chem. C.* 2013, 117(1):187–193.
- [32] Hugosson HW, Eriksson O, Jansson U, Johansson B. Phase stabilities and homogeneity ranges in 4d-transition-metal carbides: a theoretical study. *Phys. Rev. B.* 2001, 63:134108.
- [33] Jiang S, Shao L, Fan T, Duan JM, Chen X, Tang B. Mechanical behavior of high entropy carbide (HfTaZrTi)C and (HfTaZrNb)C under high pressure: Ab initio study. *Int. J. Quantum Chem.* 2020, 121(5).
- [34] Ning S, Wen T, Ye B, Cji YH. Low-temperature Molten salt synthesis of high-entropy carbide nanopowders. *J. Am. Ceram. Soc.* 2020(103):2244–2251.
- [35] Bérardan D, Franger S, Dragoë D, Meena AK, Dragoë N. Colossal dielectric constant in high entropy oxides. *Phys. Status Solid.* 2016, 10(4):328–333.
- [36] Silvestroni L, Pienti L, Guicciardi S, Sciti D. Strength and toughness: the challenging case of tac-based composites. *Compos. Part B.* 2015, 72:10–20.
- [37] Liu Y, Liang J, Guo W, Sun S, Tian Y, *et al.* Cr-assisted low-temperature densification of (Ti,Zr,Nb,Ta,Mo)C high-entropy carbides with ultrafine grain and enhanced hardness. *J. Adv. Ceram.* 2024, 13(6):780–788.
- [38] Ding J, Inoue A, Han Y, Kong F, Zhu S, *et al.* High entropy effect on structure and properties of (Fe, Co, Ni, Cr)-B amorphous alloys. *J. Alloys Compd.* 2017, 696:345–352.
- [39] Wang F, Inoue A, Kong F, Han Y, Zhu S, *et al.* Formation, thermal stability and mechanical properties of high entropy (Fe, Co, Ni, Cr, Mo)-B amorphous alloys. *J. Alloys Compd.* 2018, 732:637–645.
- [40] Gonze X, Amadon B, Anglade PM, Beuken JM, Bottin F, *et al.* ABINIT: First-principles approach

- to material and nanosystem properties. *Comput. Phys. Commun.* 2009, 180(12):2582–2615.
- [41] Hohenberg P, Kohn W. Inhomogeneous Electron Gas. *Phys. Rev.* 1964, 136(3B):B864.
- [42] Kresse G, Furthmüller J. Efficient iterative schemes for Ab initio total-energy calculations using a planewave basis set. *Phys. Rev. B.* 1996, 54(16):11169–11186.
- [43] Blöchl PE. Projector augmented-wave method. *Phys. Rev. B.* 1994, 50(24):17953.
- [44] Kohn W, Sham LJ. Self-consistent equations including exchange and correlation effects. *Phys. Rev.* 1965, 140:A1133–A1138.
- [45] Zhang B, Wu Y, Hui X. Progress and prospect of the first-principles calculations of high entropy carbide ceramics. *Artif. Intell. Secur.* 2024, 3(2):87–95.
- [46] Ouyang ZY, Li Y, Jin N, Ye J, Zhong Y. Anionic vacancy filled-up mechanism in $(\text{Ti}_{0.2}\text{V}_{0.2}\text{Nb}_{0.2}\text{Ta}_{0.2}\text{W}_{0.2})\text{C}_x$ high-entropy carbide. *J. Eur. Ceram. Soc.* 2024, 45(2):116887.
- [47] Yang Y, Wnag W, Gan G, Shi X, Tang B. Structural, mechanical and electronic properties of $(\text{TaNbHfTiZr})\text{C}$ high entropy carbide under Pressure: Ab initio investigation. *Physica B.* 2018, 550:163–170.
- [48] Xiong K, Wang B, Sun Z, Li W, Cheng C, *et al.* First-principles prediction of elastic, electronic, and thermodynamic properties of high entropy carbide ceramic $(\text{TiZrNbTa})\text{C}$. *Rare Metals.* 2022, 41(03).
- [49] Liu Y, Yu H, Meng H, Chu Y. Atomic-level insights into the initial oxidation mechanism of high entropy diborides by first-principles calculations. *J. Materiomics.* 2024, 10(2):423–430.
- [50] Liu S, Zhang S, Liu S, Li D, Li Y, *et al.* Phase stability, mechanical properties and melting points of high-entropy quaternary metal carbides from first-principles. *J. Eur. Ceram. Soc.* 2021, 41(13):6267–6274.
- [51] Hossain MD, Borma T, Kuma A, Chen X, Khosravani A, *et al.* Carbon stoichiometry and mechanical properties of high entropy carbides. *Acta Mater.* 2021, 251:117501.
- [52] Gonze X, Beuken JM, Caracas R, Detraux F, Fuchs M, *et al.* First-principles computation of material properties: the ABINIT software project. *Comp. Mater. Sci.* 2002, 25(3):478–492.
- [53] Liu T, Lei LW, Zhang JY, Li N. Unveiling the transporting mechanism of $(\text{Ti}_{0.2}\text{Zr}_{0.2}\text{Nb}_{0.2}\text{Hf}_{0.2}\text{Ta}_{0.2})\text{C}$ at room temperature. *Crystals.* 2023, 13(4):708.
- [54] Shi S, Xu J, Cui Y, Lu X, Ouyang CY, *et al.* Multiscale materials computational methods. *Sci. Technol. Review.* 2015, 33(10):20–30.
- [55] Ye B, Wen T, Huang K, Wang C, Chu Y. First-principles study, fabrication and characterization of $(\text{Hf}_{0.2}\text{Zr}_{0.2}\text{Ta}_{0.2}\text{Nb}_{0.2}\text{Ti}_{0.2})\text{C}$ high-entropy ceramic. *J. Am. Ceram. Soc.* 2019,102(7): 4344–4352.
- [56] Feng X, Wang X, Wu L, Chai B, Fu L. The effects of refractory elements on the properties of quaternary high entropy carbides-a first-principles and experiment study. *Comp. Mater. Sci.* 2024, 245:1–13.
- [57] Li Z, Wang Z, Wu Z, Xu B, Zhao S, *et al.* Phase, microstructure and related mechanical properties of a series of $(\text{NbTaZr})\text{C}$ -based high entropy ceramics. *Ceram. Int.* 2021, 47(10A):14341–14347.
- [58] Liu Y, Zhu Z, Tang Z, Yu H, Zhuang L, *et al.* Unraveling lattice-distortion hardening mechanisms in high-entropy carbides. *Small.* 2024, 20:2403159.
- [59] Ma L, Wang Z, Huang J, Huang G, Xue M, *et al.* Effect of alloying elements on stacking fault energies and twinnabilities in high-entropy transition-metal carbides. *J. Am. Ceram. Soc.* 2021, 104:6521–6532.

- [60] Shulumba N, Hellman O, Raza Z, Alling B, Barrirero J. Lattice vibrations change the solid solubility of an alloy at high temperatures. *Phys. Rev. Lett.* 2016, 117:205502.
- [61] Rogal L, Bobrowski P, Kormann F, Divinski S, Stein F, *et al.* Computationally-driven engineering of sublattice ordering in a hexagonal AlHfScTiZr high entropy alloy. *Sci. Rep.* 2017, 7(1):2209.
- [62] Wang G, Xu J, Peng S, Xie Z, Munroe P. High-entropy carbides designed to resist cavitation erosion-corrosion in an acidic environment: surface engineering guided by first-principles calculations and experiments. *Vacuum.* 2023, 211:111974.
- [63] Jiang S, Lin S, Fan T, Duan J, Chen X, *et al.* Elastic and thermodynamic properties of high entropy carbide (HfTaZrTi)C and (HfTaZrNb)C from Ab initio investigation. *Ceram. Int.* 2020, 46(10):15104–15112.
- [64] Zhou C, Zhou Y, Xing X, Liu S, Ren X, *et al.* Precipitation stability and micro-property of (Nb, Ti)C carbides in MMC coating. *J. Alloys. Compd.* 2018, 763:670–678.
- [65] Zhang Q, Zhang J, Li N, Chen W. Understanding the electronic structure, mechanical properties, and thermodynamic stability of (TiZrHfNbTa)C combined experiments and first-principles simulation. *J. Appl. Phys.* 2019, 126(2):025101–025101.
- [66] Zhao S. Lattice distortion in high-entropy carbide ceramics from first principles calculations. *J. Am. Ceram. Soc.* 2021, 104(4):1874–1886.
- [67] Shulumba N, Hellman O, Raza Z, Alling B, Barrirero J. Lattice vibrations change the solid solubility of an alloy at high temperatures. *Phys. Rev. Lett.* 2016, 117:205502.
- [68] Gao P. Atomic scale research on component optimization and point defect properties of transition metal carbide high entropy ceramics (in Chinese). *Harbin: Harbin Institute of Technology* 2022.
- [69] Guan S, Liang H, Wang Q, Tan L, Peng F. Synthesis and phase stability of the high-entropy carbide (Ti_{0.2}Zr_{0.2}Nb_{0.2}Ta_{0.2}Mo_{0.2})C under extreme conditions. *Inorg. Chem.* 2021, 60(6):3807–3813.
- [70] Abujafar MS, Leonhardi V, Jaradat R, Mousa AA, Al-qaisi S, *et al.* Structural, electronic, mechanical, and dynamical properties of scandium carbide. *Results Phys.* 2021, 21:103804.
- [71] Liu S, Zhang S, Liu S, Li D, Niu Z, *et al.* Stability and mechanical properties of single-phase quinary high-entropy metal carbides: first-principles theory and thermodynamics. *J. Eur. Ceram. Soc.* 2022, 42(7):3089–3098.
- [72] Zhang B, Wu Y, Hui X. Progress and prospect of the first-principles calculations of the compound high entropy carbide ceramics. *Artif. Intell. Secur.* 2024, 3(2):87–95.
- [73] Sangiovanni DG, Tasnádi F, Harrington T, Harrington T, Oden M, *et al.* Temperature-dependent elastic properties of binary and multicomponent high-entropy refractory carbides. *Mater. Design.* 2021, 204:109634.
- [74] Li C, Fu T, Hu H, Shen X, Hu H, *et al.* Mechanical response and grain boundary behavior of (HfNbTaTiZr)C high-entropy carbide ceramics and its constituent binary carbides. *Surf. Interfaces.* 2024, 52:104982.
- [75] Daoud S, Bouarissa N, Benmakhlouf A, Allaoui O. High-pressure effect on elastic constants and their related properties of MgCa intermetallic compound. *Phys. Status Solidi B.* 2020, 257:1900537.
- [76] Huang B, Duan Y, Sun Y, Peng M, Chen S. Electronic structures, mechanical and thermodynamic properties of cubic alkaline-earth hexaborides from first principles calculations. *J. Alloys. Compd.* 2015, 635:213–224.
- [77] Grimvall G, Magyari-köpe B, Ozolinš ENM, Persson KA. Lattice instabilities in metallic elements.

- Rev. Mod. Phys.* 2012, 84(2):945–986.
- [78] Chung DH, Buessem WR. The voigt-reuss-hill approximation and elastic moduli of polycrystalline MgO, CaF₂, b-ZnS, ZnSe, and CdTe. *J. Appl. Phys.* 1967, 38:2535–2540.
- [79] Zhao S. Lattice distortion in high-entropy carbide ceramics from first-principles calculations. *J. Am. Ceram. Soc.* 2021, 104(4):1874–1886.
- [80] Zhang P, Ye L, Chen F, Han W, Wu Y, *et al.* Stability, mechanical, and hermodynamic behaviors of (TiZrHfTaM)C (M = Nb, Mo, W, V, Cr) high-entropy carbide ceramics. *J. Alloys. Compd.* 2022, 903:163868.
- [81] Li C, Fu T, Hu H, Duan M, Weng S, *et al.* Designing the mechanical behavior of (HfTiZr)_{1-x}(NbTa)_xC high-entropy carbide ceramics. *Phys. Rev. B.* 2024, 109:134110.